



# NF $\kappa$ B/Orai1 Facilitates Endoplasmic Reticulum Stress by Oxidative Stress in the Pathogenesis of Non-alcoholic Fatty Liver Disease

Bingbing Zhang<sup>1†</sup>, Ming Li<sup>2†</sup>, Ying Zou<sup>2</sup>, Han Guo<sup>2</sup>, Bingdong Zhang<sup>3</sup>, Cheng Xia<sup>2</sup>, Hongyou Zhang<sup>2</sup>, Wei Yang<sup>2</sup> and Chuang Xu<sup>2\*</sup>

<sup>1</sup> College of Life Science and Technology, Heilongjiang Bayi Agricultural University, Daqing, China, <sup>2</sup> College of Animal Science and Technology, Heilongjiang Bayi Agricultural University, Daqing, China, <sup>3</sup> Luquan No.3 Hospital, Shijiazhuang, China

## OPEN ACCESS

### Edited by:

Simon Rousseau,  
McGill University, Canada

### Reviewed by:

Huijun Sun,  
Dalian Medical University, China  
Irene Crespo,  
University of León, Spain

### \*Correspondence:

Chuang Xu  
xuchuang7175@163.com

<sup>†</sup> These authors have contributed  
equally to this work

### Specialty section:

This article was submitted to  
Signaling,  
a section of the journal  
Frontiers in Cell and Developmental  
Biology

**Received:** 25 June 2019

**Accepted:** 05 September 2019

**Published:** 02 October 2019

### Citation:

Zhang B, Li M, Zou Y, Guo H,  
Zhang B, Xia C, Zhang H, Yang W and  
Xu C (2019) NF $\kappa$ B/Orai1 Facilitates  
Endoplasmic Reticulum Stress by  
Oxidative Stress in the Pathogenesis  
of Non-alcoholic Fatty Liver Disease.  
*Front. Cell Dev. Biol.* 7:202.  
doi: 10.3389/fcell.2019.00202

Non-esterified fatty acids (NEFAs) promote *de novo* lipogenesis, which caused abnormal hepatic lipid accumulation, by the NF $\kappa$ B–Orai1 pathway. Oxidative stress and endoplasmic reticulum (ER) stress have been recognized as key mechanisms in non-alcoholic fatty liver disease (NAFLD) pathogenesis. Whether Orai1 facilitates ER stress by oxidative stress remains unknown. The rat model of NAFLD was constructed by feeding high-fat diet (HFD). BRL-3A cells were treated with NEFAs, Orai1 inhibitor BTP2, NF $\kappa$ B inhibitor wogonin, or small interfering Orai (siOrai) 1, respectively. The content of intracellular reduced glutathione (GSH) and malondialdehyde (MDA), indicating oxidative stress, was measured by a spectrophotometer. ER stress major proteins PERK, IRE1, ATF6, CHOP, and GRP78 were quantified using Western blot and qRT-PCR analyses. For the intracellular location of reactive oxygen species (ROS) and Orai1 were measured by Western blot and immunofluorescence, and cytosolic Ca<sup>2+</sup> was measured by flow cytometry. As we expected, the liver of rats with NAFLD showed lipid droplets in HE and Oil Red O. The decreased GSH and increased MDA were found in rats fed with HFD. ER stress major proteins PERK, IRE1, ATF6, GRP78, and CHOP were significantly increased in the HFD group. In BRL-3A cells, GSH content dramatically decreased from 1 h, MDA content dramatically increased from 3 h, and expression levels of ER stress significantly increased from 3 h by NEFA treatment. Furthermore, cytosolic Ca<sup>2+</sup> increased from 0.5 h by NEFAs treated in BRL-3A cells. It indicated that NEFAs increased cytosolic Ca<sup>2+</sup> to induce oxidative stress, thus ER stress. The content of oxidative stress and ER stress proteins showed the same trends by NEFAs treated in BRL-3A cells. These effects were reversed by the Orai1 inhibitor BTP2 and the NF $\kappa$ B inhibitor wogonin. Moreover, siOrai1 abrogated NEFAs' influence in BRL-3A cells. Last, ROS was found by NEFAs treated in BRL-3A cells, and NEFA treatment enhanced the nuclear localization of NF- $\kappa$ B p65 and ORAI1. It was considered that high NEFAs increased cytosolic Ca<sup>2+</sup> and enhanced NF $\kappa$ B-dependent SOCE and its moiety protein Orai1 to decrease GSH and thus induced oxidative stress at earlier stages and furthermore tempted ER stress in the pathologic progress of NAFLD.

**Keywords:** NAFLD, oxidative stress, ER stress, Orai1, NEFA

## INTRODUCTION

Non-alcoholic fatty liver disease (NAFLD) is a common chronic health problem with increasing prevalence worldwide and progresses to non-alcoholic steatohepatitis, cirrhosis, obesity, and type II diabetes in both adults and children. The pathological characterizations of NAFLD are aberrant lipid accumulation, inflammation, and fibrotic scarring in liver. Moreover, basic and clinical evidence indicated that NAFLD has a strong relationship to insulin resistance. The two-hit model is the most widespread and prevailing theory of NAFLD. The first hit is insulin resistance, which leads to hepatic fat accumulation; the second hit is regulation of free fatty acids by the adipokines (leptin, adiponectin, resistin) to induce mitochondrial dysfunction and oxidative stress (Zeng et al., 2014). High-plasma non-esterified fatty acids (NEFAs) level is a pathological characteristic of NAFLD, obesity, and metabolic syndrome (Engin, 2017). NEFAs are any fatty acids (above C10), rather than being esterified with glycerol to form a glyceride or other lipid. Plasma NEFAs mainly include palmitic acid, palmitoleic acid, stearate, oleic acid, and linoleic acid (Diraison et al., 2003; Donnelly et al., 2005; Hetherington et al., 2016).

Previous studies have shown that NEFAs induced oxidative stress and endoplasmic reticulum (ER) stress in hepatocyte and mammary epithelial cells (Cao and Kaufman, 2014; Hasnain et al., 2016). Oxidative stress contributes to many pathological conditions, including cancer, neurological disorders, atherosclerosis, hypertension, and diabetes (Joy et al., 2017; Su et al., 2018). However, oxidative stress can be beneficial due to the attack and destruction of pathogens by the immune system (Ortiz de Orue Lucana et al., 2012). While short-term oxidative stress could prevent aging, long-term effects are caused by damage to DNA, which is induced by ionizing radiation (Czerwinska et al., 2018). Reactive oxygen species (ROS), the second signal of activating NF $\kappa$ B pathway, could promote the synthesis and release of inflammation cytokines in hepatocytes to induce hepatocyte inflammation response. However, to the best of our knowledge, the role of high plasma NEFAs in affecting oxidative and ER stress has not been elucidated to date.

Intracellular Ca<sup>2+</sup> as the important second messenger participates in cell proliferation, differentiation, migration, muscular contraction, hormone secretion, glycogen metabolism, and neuronal excitation. The homeostasis of calcium, from calcium store in ER, plays key roles in ER protein folding, mutual transport and secretion, and lipid metabolism. Previous reports indicated that insulin resistance caused Ca<sup>2+</sup> concentration to increase, creating a vicious circle and promoting the pathological process of NAFLD. ER also plays key roles in reduction–oxidation balance and lipid biosynthesis. Intracellular Ca<sup>2+</sup> and ROS are sensitive to protein folding in the ER. The role of cytosolic Ca<sup>2+</sup> in oxidative stress and ER stress is unclear. In certain cell types, Ca<sup>2+</sup> may enter through the SOCE (store-operated Ca<sup>2+</sup> entry) moiety Orai1 (Prakriya et al., 2006). Notably, the expression of Orai1 has previously been shown to be regulated by nuclear factor NF $\kappa$ B

(Lang and Shumilina, 2013). The present study addresses the question of whether Orai1 facilitates ER stress by oxidative stress in the pathogenesis of NAFLD.

## MATERIALS AND METHODS

### Animal Experiments and Samples Collection

The animal experiments were performed in accordance with the Guiding Principles of Animals adopted by the Chinese Association for Laboratory Animal Sciences for the welfare of animals. The present study protocol was approved by the Ethics Committee for the Use and Care of Animals, Heilongjiang Bayi Agricultural University (Daqing, China). For our study, 18 rats 6–8 weeks of age had free access to food and tap water, and randomly divided into two groups. The nine rats of the high-fat diet (HFD) group were fed a HFD containing 70% kcal from fat (Altromin, Shanghai, China) for 8 weeks to induce NAFLD. The nine rats of the control group were fed normal chow. All animals had free access to food and tap water. Part of the liver was collected and immediately shock-frozen in liquid nitrogen and lysed in lysis buffer for Western blots, GSH, and MDA measurements, and another for H&E and Oil Red staining. The blood was collected from postcaval vein to measure non-esterified free fatty acids through the Non-esterified Free fatty acids kit (Beijing Jiuqiang Biotechnology Co., Ltd., Beijing, China) with an automatic clinical analyzer (Synchron DXC800; Beckman Coulter, Inc., Brea, CA, United States).

### Cell Culture

BRL-3A rat liver cells were obtained from ATCC and cultured in DMEM high-glucose medium (Gibco, Shanghai, China) supplemented with 10% FBS (Clark, Australia) and 1% penicillin (100 U/mL)/streptomycin (100  $\mu$ g/mL) liquid (Solarbio, Beijing, China) at a 37°C incubator with 5% CO<sub>2</sub>. Cells were treated with 1.2 mM NEFAs for different time durations or treated with vehicle only.

Cells were pretreated with 20  $\mu$ M CRAC Channel Inhibitor BTP2 (Sigma, Shanghai, China) and 100  $\mu$ M NF $\kappa$ B inhibitor wogonin (Sigma) or treated with vehicle only. After 12 h, cells were in addition treated with 1.2 mM NEFAs for 12 h.

### Prepared NEFAs

The composition and concentration of NEFAs used in this study were according to previous descriptions (Li et al., 2013; Abdelmagid et al., 2015; Plos One Staff, 2015; Zhang et al., 2018).

### Silencing

For silencing,  $3 \times 10^5$  cells (6-well plate) were seeded and incubated in antibiotic-free medium for 24 h before silencing treatment. Afterward, cells were transfected with 40 pM rat Orai1 siRNA (GenePharma, Shanghai, China) and non-targeting siRNA (GenePharma, Shanghai, China) using

Lipofectamine 2000 Transfection Reagent (Invitrogen, Shanghai, China) according to the manufacturer's protocol<sup>1</sup>.

## Quantification of mRNA Expression

Total RNA was extracted from BRL-3A cells of the above treatments with Trizol RNA extraction reagent (Invitrogen Corporation, Carlsbad, CA, United States); mRNA transcription and cDNA synthesis were performed with Reverse Transcriptase M-MLV (RNase H-) (Takara Bio, Beijing, China) using an oligodT18 primer. Quantitative RT-PCR was performed by FastStart Universal SYBR Green Master (F. Hoffmann-La Roche AG, Basel, Switzerland) under the following conditions: 95°C for 3 min, followed by 40 cycles at 95°C for 10 s and 58°C for 30 s on a BioRad iCycler iQTM Real-Time PCR Detection System (Bio-Rad Laboratories Inc., Hercules, CA, United States). Calculated rat Orai1 and Grp78 mRNA expression were quantified with the  $2^{-\Delta\Delta CT}$  method and normalized to TATA box-binding protein (Tbp).

The following primers were used:

*Rat Tbp* (TATA box-binding protein):

forward (5'-3'): ACTCCTGCCACACCAGCC

reverse (5'-3'): GGTCAAGTTTACAGCCAAGATTCA

<sup>1</sup>[https://www.thermofisher.com/document-connect/document-connect.html?url=https%3A%2F%2Fassets.thermofisher.com%2Fassets%2Fmanuals%2FLipofectamine\\_2000\\_Reag\\_protocol.pdf&title=TGlwb2ZlY3RhbWluZSZyZWc7IDIwMDAgUmVhZ2VudCBQcm90b2NvbA==](https://www.thermofisher.com/document-connect/document-connect.html?url=https%3A%2F%2Fassets.thermofisher.com%2Fassets%2Fmanuals%2FLipofectamine_2000_Reag_protocol.pdf&title=TGlwb2ZlY3RhbWluZSZyZWc7IDIwMDAgUmVhZ2VudCBQcm90b2NvbA==)

## Rat Orai1

forward (5'-3'): CGTCCACAACCTCAACTCC

reverse (5'-3'): AACTGTCCGGTCCGTCTTAT

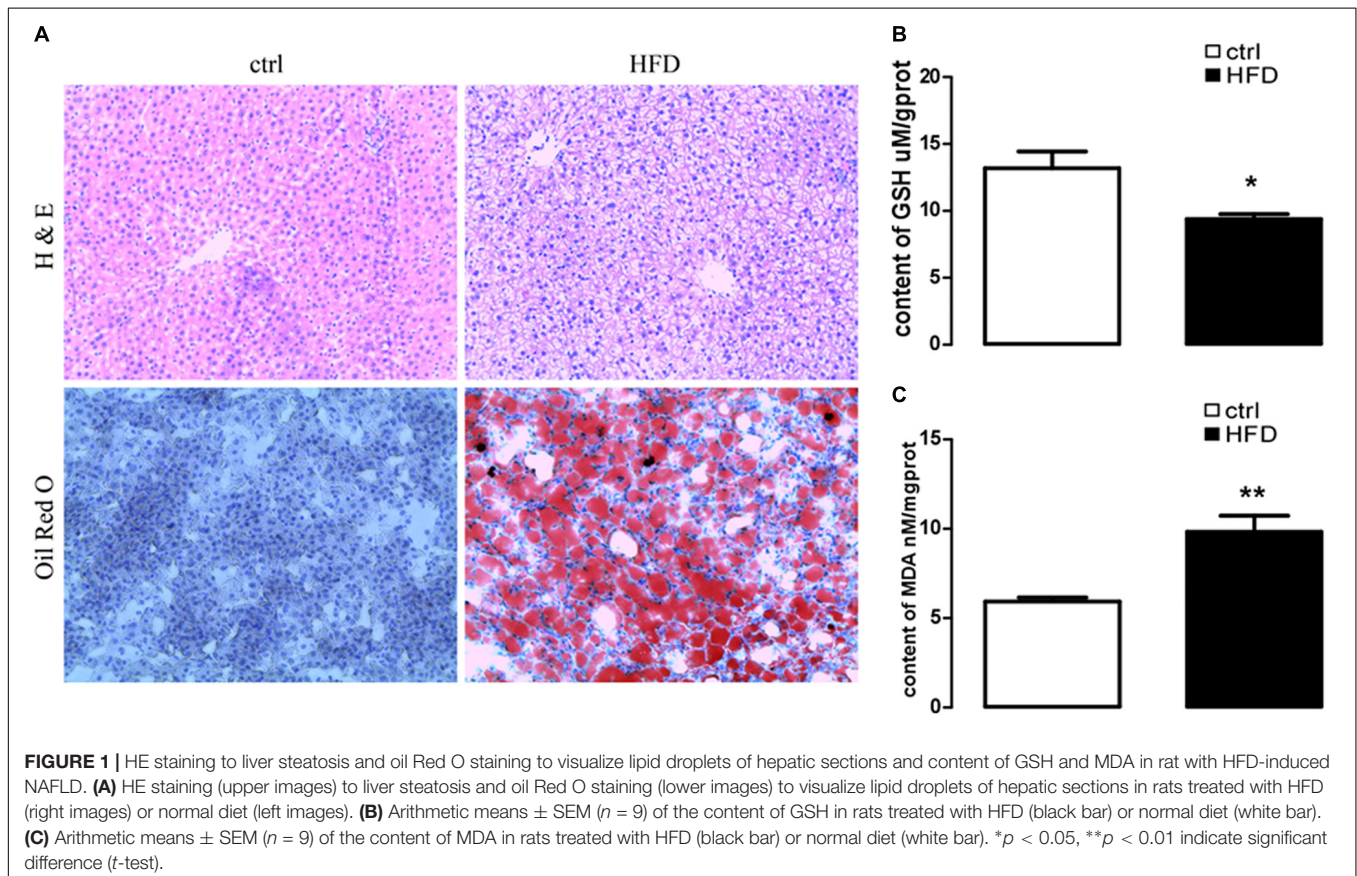
## Rat Grp78

forward (5'-3'): AACCCAGATGAGGCTGTAGCATA

reverse (5'-3'): CACAGTGTTCCTCGGAATCAGTT

## Western Blotting

PERK, IRE1, ATF6, GRP78, CHOP, Orai1, NF-κB p65, and β-actin protein levels were determined in rat livers and BRL-3A cells. The samples with RIPA lysis buffer (Beyotime Biotechnology, Shanghai, China) were incubated on ice for 30 min and later centrifuged at 14,000 rpm for 20 min (4°C). Total protein was collected and separated by SDS-PAGE and subsequently transferred to PVDF membranes and blocked in 5% non-fat milk/Tris-buffered saline/Tween-20 (TBST) at room temperature for 1 h. Membranes were incubated overnight at 4°C with polyclonal rabbit anti-PERK antibody (1:1000 in 5% BSA in TBST, Cell signaling), rabbit anti-IRE1 antibody (1:1000 in 5% BSA in TBST, abcam), rabbit anti-ATF6 antibody (1:1000 in 5% BSA in TBST, abcam), mouse anti-GRP78 antibody (1:250 in 5% BSA in TBST, Santa Cruz Biotechnology), mouse anti-CHOP antibody (1:1000 in 5% BSA in TBST, Cell signaling), mouse anti-Orai1 antibody (1:1000 in 5% BSA in TBST, Cell signaling), and mouse anti-NF-κB p65 antibody (1:1000 in 5% BSA in TBST, Cell signaling). After incubation



with HRP-labeled goat anti-rabbit/mice secondary antibody (3:5000, Beyotime Biotechnology) for 1 h at room temperature, the bands were visualized with enhanced chemiluminescence reagents (Beyotime). Densitometric analysis was performed using ImageJ software. The protein expressions were quantified and normalized to  $\beta$ -actin antibody (3:5000, Cell signaling).

## Measurement of Intracellular Micro-Reduced Glutathione (GSH) and Malondialdehyde (MDA)

The contents of intracellular GSH and MDA were determined by a micro-reduced GSH test kit (Nanjing Jiancheng, China)

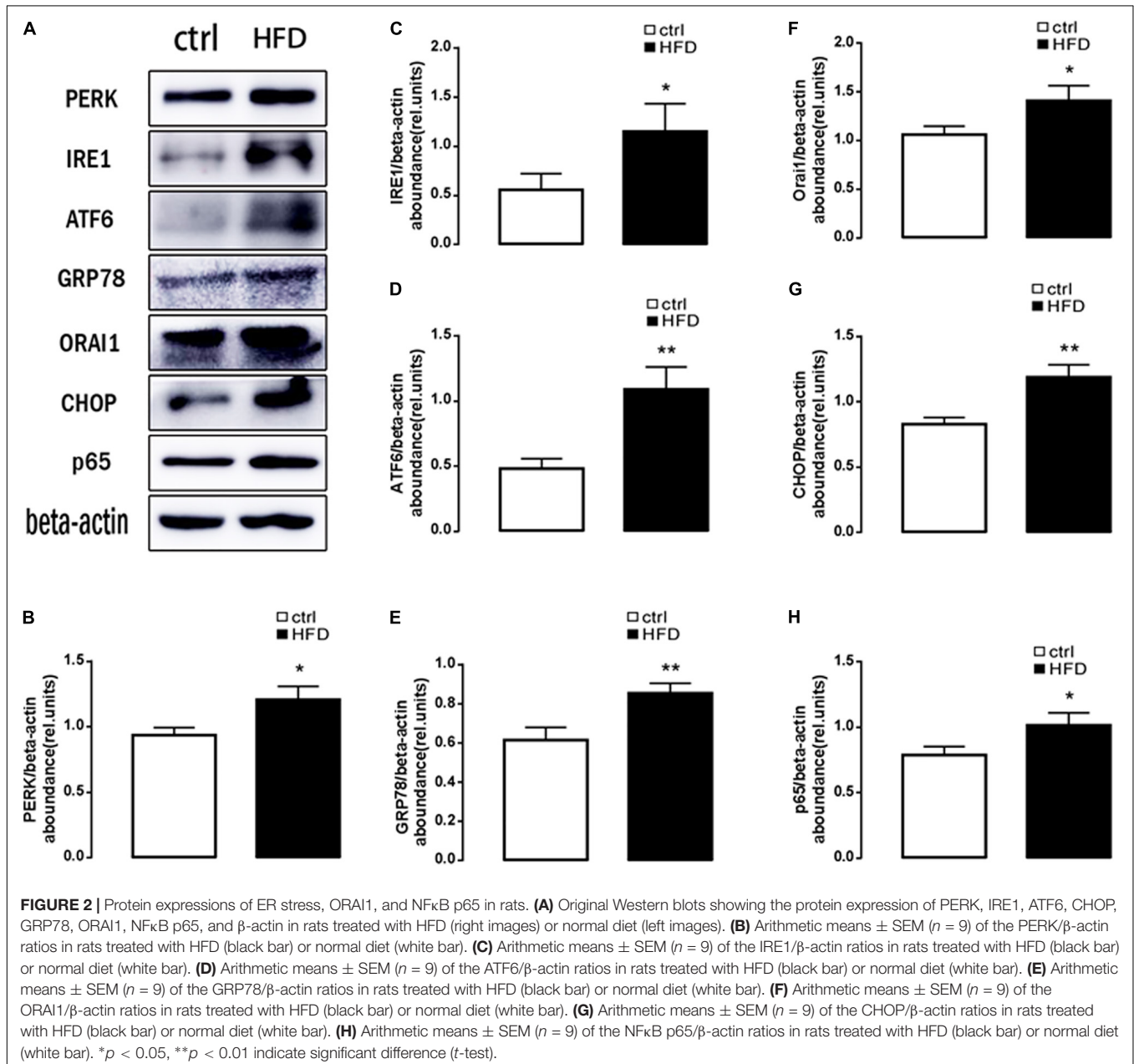
and an MDA assay kit (Beyotime Biotechnology), respectively. Briefly, the intracellular reduced GSH and MDA were measured by a spectrophotometer (Synergy neo HTS multi-mode microplate reader, BioTek) at 405 or 532 nm according to the manufacturer's instructions<sup>2,3</sup>.

## Measurement of ROS

A ROS assay kit (Beyotime) was used to determine the intracellular change in ROS generation in BRL-3A cells. A total

<sup>2</sup><http://www.njjcbio.com/products.asp?id=1532>

<sup>3</sup><https://www.beyotime.com/product/S0131.htm>



of  $1 \times 10^5$  cell samples were incubated with  $10 \mu\text{M}$  carboxy-2',7'-dichloro-dihydro-fluorescein diacetate (DCFHDA) probe to detect intracellular ROS in PBS for 15 min at  $37^\circ\text{C}$ . Fluorescence was measured at 488 nm (excitation) and 525 nm (emission) by a confocal laser-scanning microscope (Leica TCS SP8; Leica, Wetzlar, Germany) with  $40 \times /1.3$  NA differential interference contrast.

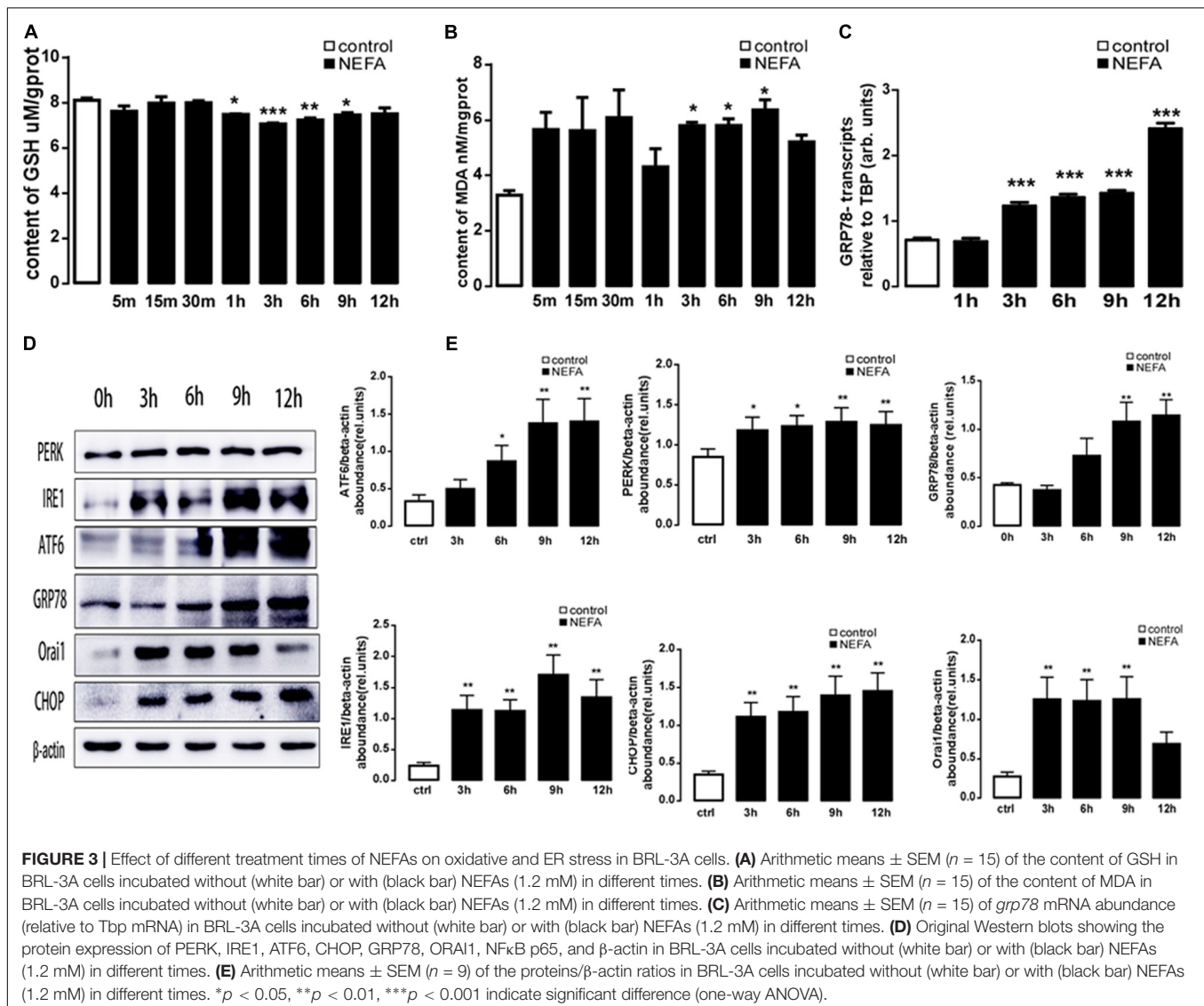
## Immunofluorescence

BRL-3A cells treated with 1.2 mM NEFAs and siOrai1 were cultured on the bottom well (Cellvis, Hangzhou, China) for 24 h and then fixed with 4% paraformaldehyde for 30 min at room temperature. BRL-3A cells were incubated with 3% Albumin Bovine V (Biosharp, Hefei, China), 5% normal goat serum (Boster, Wuhan, China), and 0.5% Triton in PBS (Biofroxx, Guangzhou, China) for 30 min at room temperature for blocking unspecific bindings. Then, rabbit anti-Orai1 and

mice anti-NF $\kappa$ B p65 were incubated in cells overnight at  $4^\circ\text{C}$  in a humidified chamber. The cells were incubated with Cy3 goat anti-rabbit IgG (1:500, Beyotime) and goat anti-mouse IgG-FITC (Santa Cruz Biotechnology) for 1 h at room temperature, respectively, after rinsing four times with PBS. The nuclei were stained with Hoechst 33342 dye (Beyotime) for 30 min at room temperature. Fluorescence and images were obtained with a confocal laser-scanning microscope (Leica TCS SP8).

## Statistics

Data are presented as the means  $\pm$  standard error of the mean (SEM) with  $n$  representing the number of independent experiments. All data were tested for significance with the unpaired Student's  $t$ -test or one-way analysis of variance (ANOVA) followed by a Tukey *post hoc* test. A probability ( $p$ ) value of  $<0.05$  was considered statistically significant.



## RESULTS

### Feeding HFD Increased Plasma NEFA Concentration to Induce NAFLD

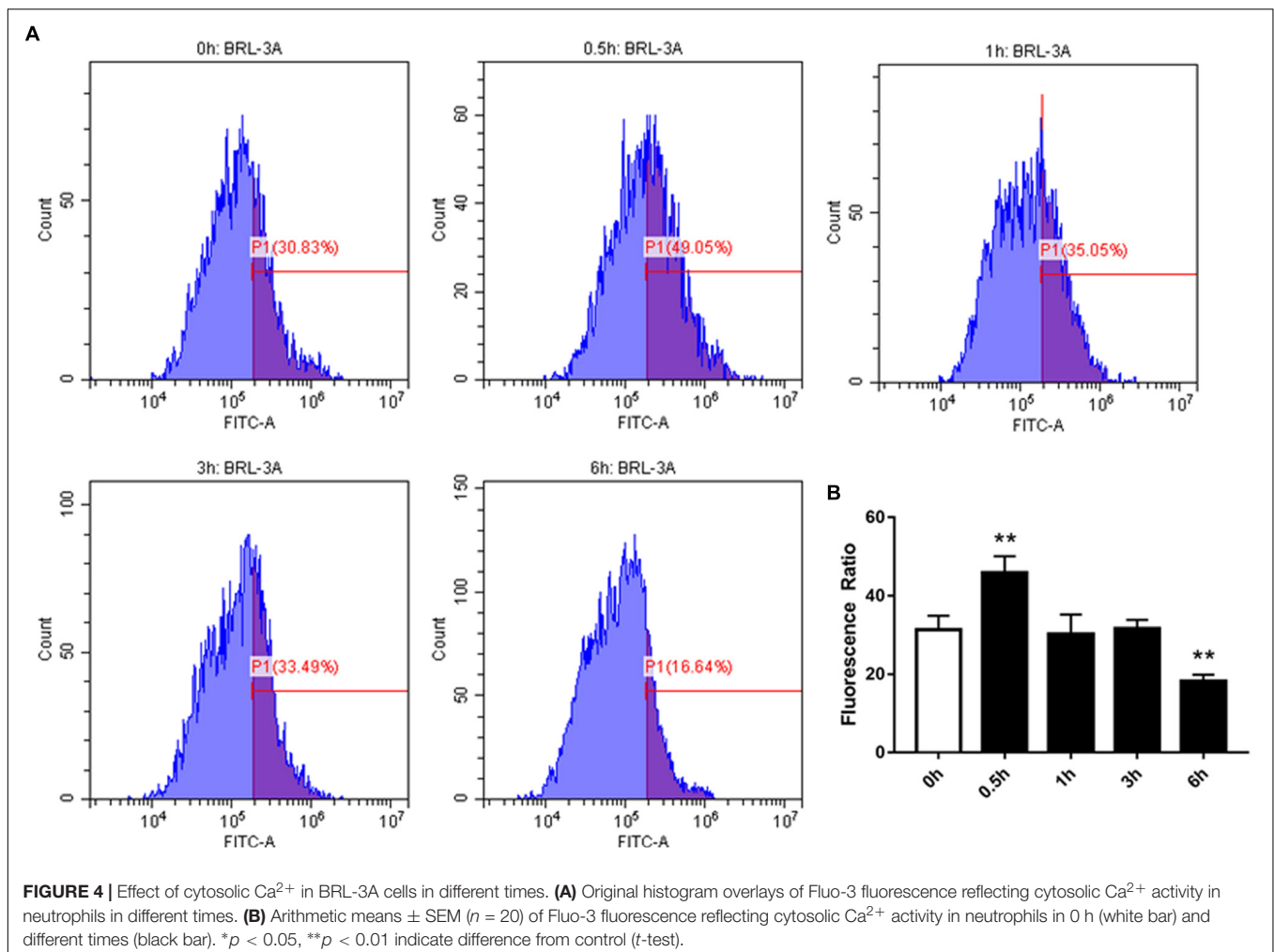
First, we addressed HFD-induced NAFLD through feeding HFD and normal diet to wild-type rats. A rat model of NAFLD was constructed according to the histopathological data. As illustrated in **Figure 1A**, severe panlobular micro- and macrovesicular steatosis were shown in the liver of the HFD group by H&E staining, and lipid drops were shown by Oil Red O staining. However, the liver of the control group showed normal hepatocytic texture with a large spherical nucleus and a homogeneous cytoplasm.

Next, plasma NEFA was measured by Non-esterified Free fatty acids assay kit, and the results showed significantly higher ( $p = 0.0073$ ) concentration in the HFD group ( $1.383 \pm 0.042$ ) than the control group ( $1.003 \pm 0.061$ ). Furthermore, GSH and MDA were measured by a spectrophotometer; protein expression of GRP78, PERK, IRE, ATF6, CHOP, Orai1, and NF $\kappa$ B p65 were measured by Western blot. As expected, the content of GSH was significantly decreased (**Figure 1B**); the content of

MDA was increased in the HFD group (**Figure 1C**). PERK, IRE, ATF6, CHOP, GRP78, Orai1, and NF $\kappa$ B p65 proteins were also dramatically increased in the HFD group compared with the control group (**Figure 2**). This result indicated that in the progress of NAFLD, plasma NEFA was associated with oxidative stress and ER stress.

### High-Concentration NEFAs Induced Oxidative Stress and ER Stress in BRL-3A Cells

To explore whether a high amount of NEFAs induced oxidative stress and ER stress, in the present study, BRL-3A cells were treated with high-concentration NEFAs to construct a NAFLD cell model (Zhang et al., 2018) to measure oxidative stress and ER stress. Initially, BRL-3A cells were treated with 1.2 mM NEFAs for 5 min, 15 min, 30 min, 1 h, 3 h, 6 h, 9 h, and 12 h to measure the content of MDA and GSH, and expression of GRP78, PERK, IRE, ATF6, and CHOP. As shown in **Figure 3**, a significant decrease in GSH level was detected from 1 to 9 h (**Figure 3A**), and content of MDA was significantly increased from 3 to 9 h (**Figure 3B**). Nevertheless, GRP78 transcription was dramatically



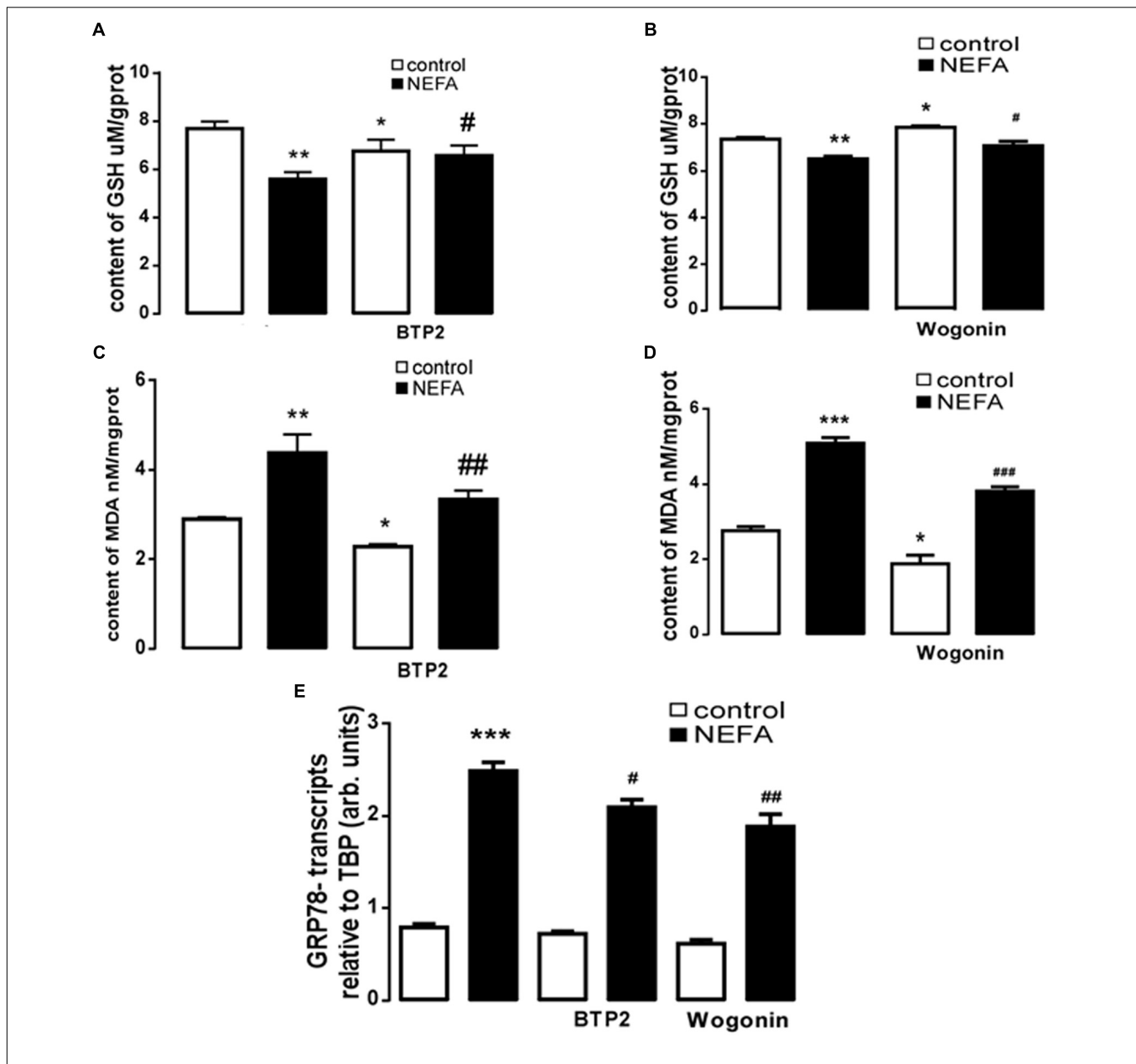
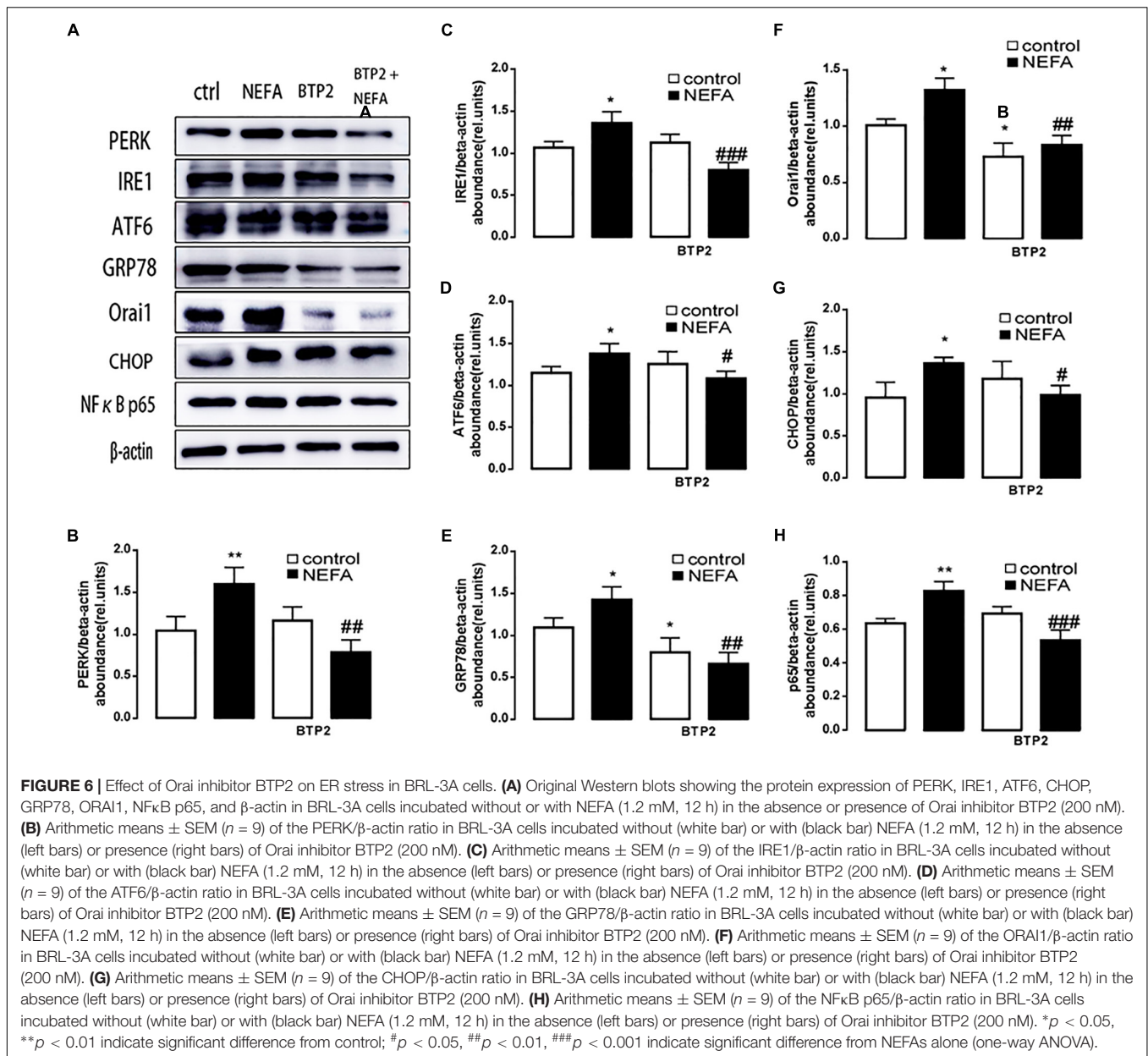


**FIGURE 5 |** Effect of NEFAs on content of MDA and GSH, transcription of GRP78 in BRL-3A cells with or without the presence of 2-APB and Wogonin. **(A)** Arithmetic means  $\pm$  SEM ( $n = 15$ ) of the content of GSH in BRL-3A cells incubated without (white bar) or with (black bar) NEFAs (1.2 mM, 3 h) in the absence (left bars) or presence (right bars) of Orai inhibitor BTP2 (200 nM). **(B)** Arithmetic means  $\pm$  SEM ( $n = 15$ ) of the content of GSH in BRL-3A cells incubated without (white bar) or with (black bar) NEFAs (1.2 mM, 3 h) in the absence (left bars) or presence (right bars) of NF $\kappa$ B inhibitor wogonin (100  $\mu$ M). **(C)** Arithmetic means  $\pm$  SEM ( $n = 15$ ) of the content of MDA in BRL-3A cells incubated without (white bar) or with (black bar) NEFAs (1.2 mM, 3 h) in the absence (left bars) or presence (right bars) of Orai inhibitor BTP2 (200 nM). **(D)** Arithmetic means  $\pm$  SEM ( $n = 15$ ) of the content of MDA in BRL-3A cells incubated without (white bar) or with (black bar) NEFAs (1.2 mM, 3 h) in the absence (left bars) or presence (right bars) of NF $\kappa$ B inhibitor wogonin (100  $\mu$ M). **(E)** Arithmetic means  $\pm$  SEM ( $n = 11$ ) of Grp78 mRNA abundance (relative to Tbp mRNA) in BRL-3A cells incubated without (white bar) or with (black bar) NEFAs (1.2 mM, 12 h) in the absence (left bars) or presence (right bars) of Orai inhibitor BTP2 (200 nM) or of NF $\kappa$ B inhibitor wogonin (100  $\mu$ M). \* $p < 0.05$ , \*\* $p < 0.01$ , \*\*\* $p < 0.001$  indicate significant difference from control; # $p < 0.05$ , ## $p < 0.01$ , ### $p < 0.001$  indicate significant difference from NEFAs alone (one-way ANOVA).

increased from 3 to 12 h (Figure 3C), and the major ER stress-related proteins levels of PERK, IRE1, ATF6, GRP78, and CHOP were significantly up-regulated from 6 to 12 h (Figures 3D,E). These findings demonstrated that high NEFAs could facilitate the ER stress-induced subsequent reactions by oxidative stress.

### Effect of High-Concentration NEFAs on SOCE Moiety Orai1 in BRL-3A Cells

We examined the effect of high-concentration NEFAs on intracellular  $\text{Ca}^{2+}$  in BRL-3A cells by Fura-3. As illustrated in Figure 4, the intracellular  $\text{Ca}^{2+}$  was found to be increased

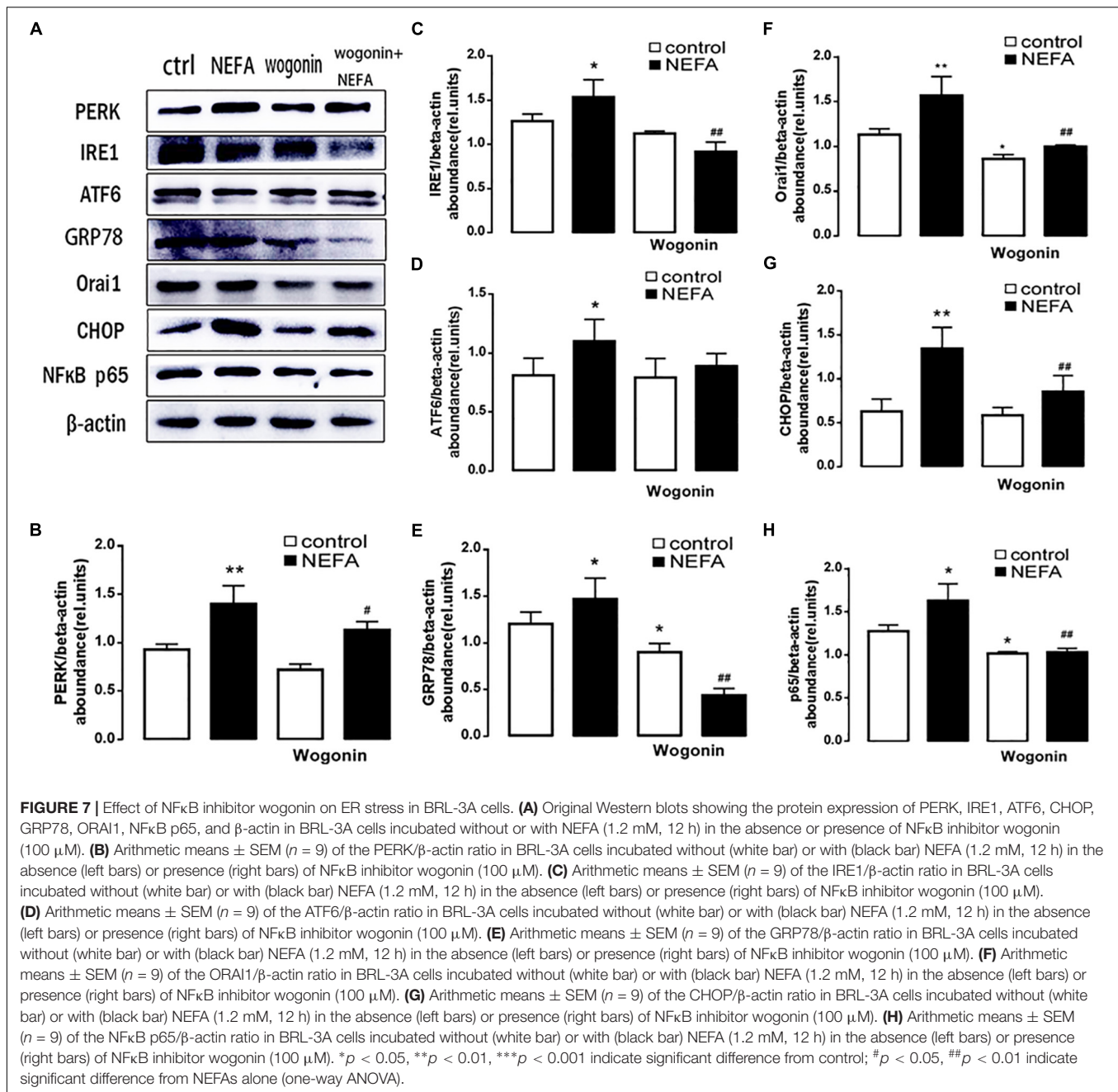


from 0.5 h in BRL-3A cells compared to the control group (Figures 4A,B). Afterward, Orai1 transcription and protein levels were increased in 3 h (Figure 3D).

In order to further explore whether high NEFAs facilitated ER stress by oxidative stress through the NFκB/Orai1 signaling pathway in BRL-3A cells, CRAC channel inhibitor BTP2 and NFκB inhibitor wogonin were used to detect the effect. We observed that GSH content was dramatically lower in the NEFA group than the control group (Figures 5A,B), and MDA was dramatically higher (Figures 5C,D). Conversely, the effects were abrogated by the BTP2 and wogonin, respectively. GRP78 mRNA level was significantly increased in the NEFA group; the effects were abrogated by BTP2 and wogonin (Figure 5E). The major ER stress-related proteins GRP78,

PERK, IRE, ATF6, and CHOP, and NFκB p65 and ORAI1 levels were significantly increased by NEFAs and BTP2 (Figures 6A–H and Supplementary Figure S1A), and wogonin (Figures 7A–H and Supplementary Figure S1B) blocked the effects of NEFA treatment.

The final series of experiments explored whether the SOCE moiety Orai1 participates in the signaling that regulates ER stress by oxidative stress. BRL-3A cells were treated with siOrai1. To verify silencing efficiency, the transcript level and protein expression of ORAI1 were quantified. As a result, the mRNA level was  $0.022 \pm 0.002$  a.u. ( $n = 9$ ) in cells transfected with siOrai1 and  $0.069 \pm 0.011$  a.u. ( $n = 9$ ),  $p < 0.01$ , in cells transfected with negative control siRNA.

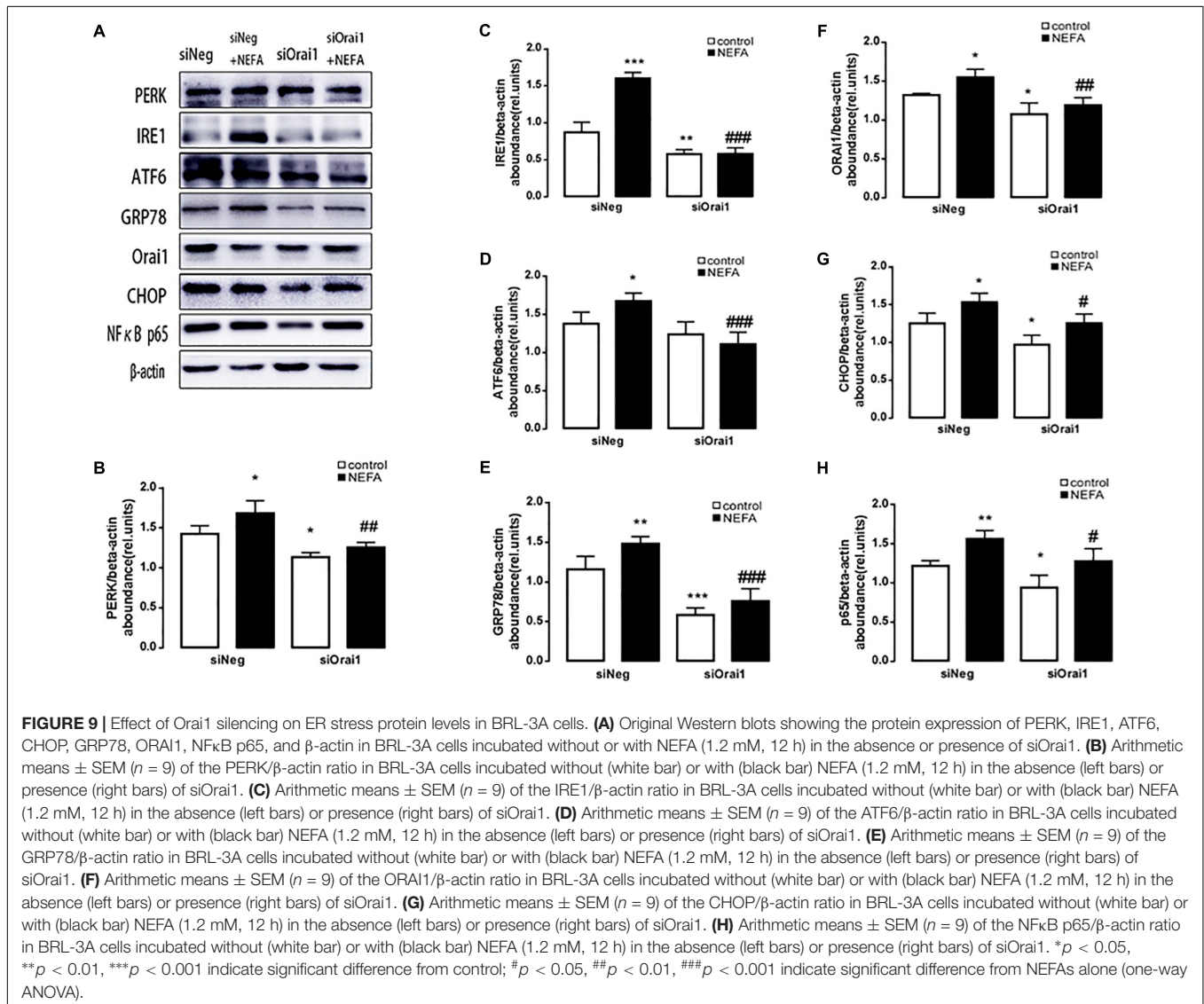
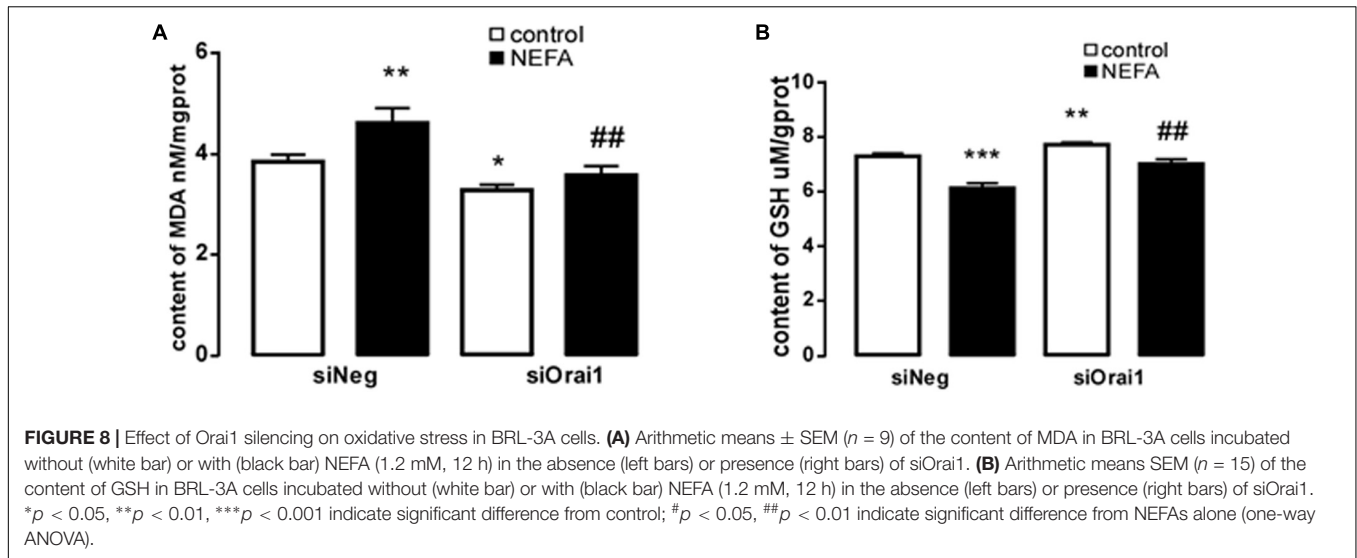


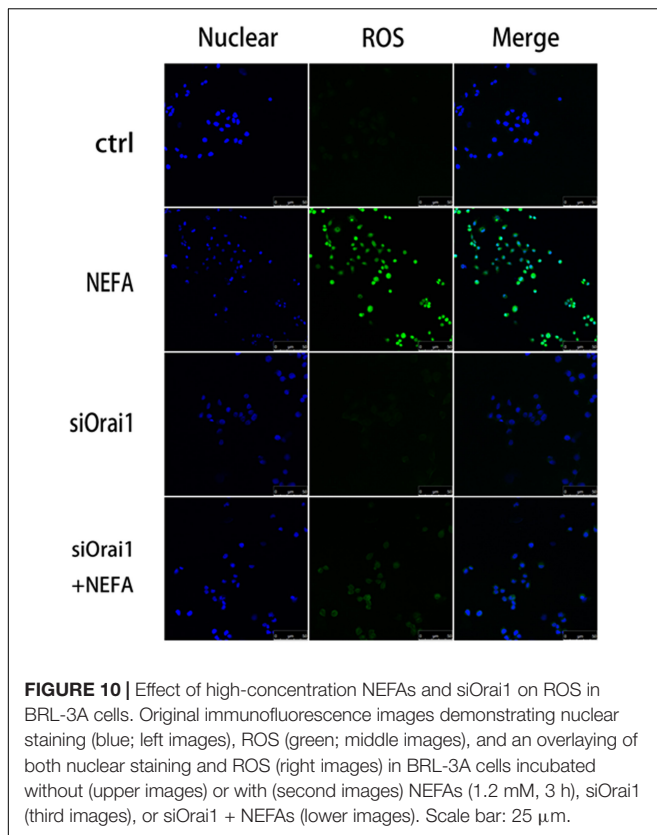
As illustrated in **Figures 8A,B**, GSH content was increased by siOrai1 and MDA content was decreased by siOrai1. As expected, the protein expression of GRP78, PERK, IRE, ATF6, and CHOP, and NFκB p65 and ORAI1 levels were dramatically decreased by siOrai1 treatment (**Figures 9A–H** and **Supplementary Figure S1C**). Furthermore, as illustrated in **Figure 10**, ROS was increased by NEFA and reduced by siOrai1. Immunofluorescence confirmed activation of Orai1, NFκB p65, and phosph-NFκB p65 by NEFAs and siOrai1 in BRL-3A cells (**Figure 11** and **Supplementary Figure S2**). These findings indicate that store-operated  $Ca^{2+}$  entry participated in NEFA-induced oxidative stress and ER stress.

## DISCUSSION

The present observations reveal an important role of the store-operated  $Ca^{2+}$  entry moiety Orai1 in the regulation of ER stress by oxidative stress in the progress of NAFLD. Furthermore, in the pathologic process of NAFLD, NEFAs facilitated ER stress by oxidative stress through NFκB-dependent Orai1 signaling in BRL-3A cells.

Oxidative stress and ER stress are highly interrelated with multiple hepatic dysfunctions, including insulin resistance, lipotoxicity, inflammation, and steatosis. Mitochondrial ROS generation plays a key role in these two hits of the NAFLD

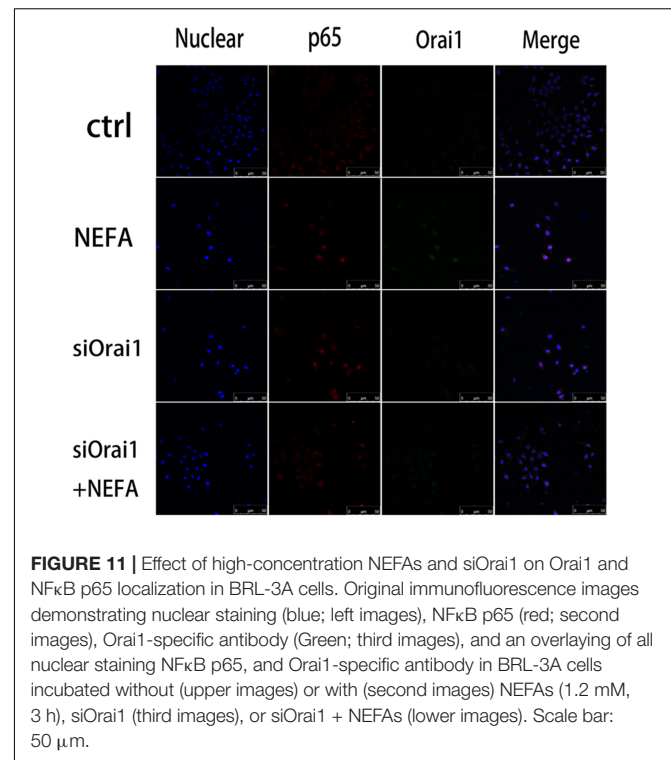




process. MDA is also a marker for oxidative stress, produced by lipid peroxidation of polyunsaturated fatty acids by ROS degradation. As a reactive aldehyde, MDA is an important reactive electrophile species that could induce toxic stress in cells and form advanced lipoxidation end products (ALE), a kind of covalent protein complex, in analogy to advanced glycation end products (AGE) (Farmer and Davoine, 2007). Furthermore, the production of MDA also indicated the level of oxidative stress in an organism (Moore and Roberts, 1998; Del Rio et al., 2005). In this research, high levels of MDA were measured after NEFA treatment for 3 h.

Glutathione is an endogenous antioxidant that protects tissues from oxidative stress by reducing hydroperoxides and organic peroxides, including lipid peroxide, protecting the cell membrane from free radical oxidative damage during redox reactions. GSH is considered to be a free radical scavenger of ROS and an inhibitor of lipid peroxidation (Owen and Butterfield, 2010). The redox function in cells protects the cell membrane from free radical oxidation damage (Zitka et al., 2012). In this research, low levels of GSH after NEFA treatment for 1 h indicated an increase in oxidative stress.

As is well-known, the pathogenic process of NAFLD is linked to aberrant lipid accumulation, insulin resistance, and inflammation in hepatocytes. Previous reports have shown that a high concentration of NEFAs has been present in human patients (Giacomini et al., 1980), as well as in cattle and animal models with NAFLD. In the present study, we added a high concentration of NEFAs into BRL-3A cell lines for different times in the pathologic process of NAFLD. The results showed that oxidative



stress appeared from 1 to 9 h, and ER stress appeared from 6 to 12 h. This finding indicates that NEFAs induced mitochondrial dysfunction and then ER stress.

ROS acts as a major regulator in the maintenance of homeostasis of ER stress involving UPR-mediated cell signaling, leading to UPR activation and restoration of ER homeostasis (Zeeshan et al., 2016). GSH plays a key role in maintaining ER oxidoreductases in a reduced state, and was considered to induce calcium release via inositol triphosphate receptors (IP3R) (Chan et al., 2016; Zeeshan et al., 2016). Enhanced mitochondrial  $\text{Ca}^{2+}$  increased metabolism activities and ROS generation in mitochondria (Gorlach et al., 2006). In this research, store-operated  $\text{Ca}^{2+}$  entry increased after NEFA treatment for 0.5 h. Therefore, we speculate that intracellular  $\text{Ca}^{2+}$  correlated with decreased GSH.

Intracellular  $\text{Ca}^{2+}$  plays an important role in signal transduction in various cell types, involving cell proliferation, cell death, migration, and metabolism (Lang et al., 2012; Ivanova et al., 2017). Orai1, the moiety of SOCE, was activated by NEFAs and facilitates  $\text{Ca}^{2+}$  entry to maintain  $\text{Ca}^{2+}$  balance. In addition, we also added  $\text{Ca}^{2+}$  inhibitor  $\text{BTP}_2$  and silencing Orai1 into BRL-3A cell lines before NEFA treatment, and the results showed that NEFA could activate mitochondrial ROS production and cause ER stress; conversely, the effects were decreased by inhibitor  $\text{BTP}_2$  and silencing Orai1. Orai1 expression was shown to be up-regulated by NF $\kappa$ B (Lang and Shumilina, 2013). The present study demonstrates that an NF $\kappa$ B inhibitor reduces Orai1 expression. Moreover, oxidative stress and ER stress were also down-regulated by the NF $\kappa$ B inhibitor wogonin. The results also showed that when Orai1 is silenced, the content of p65 translocated to the nucleus could be reduced. This suggests that

Orai1 may interact with p65. Thus, we suspect that it may be effective in inflammation after silencing Orai1. The present observations, however, do not rule out that NF $\kappa$ B could play a permissive role in the regulation of oxidative stress and ER stress in the pathologic process of NAFLD. The NF $\kappa$ B–Orai1 pathway plays an important role in the inflammatory responses that regulate hepatic lipid deposition in the pathological process of NAFLD. Inhibition of the NF $\kappa$ B–Orai1 pathway could reduce NEFA-induced oxidative stress, thus decreasing ER stress and causing NAFLD. Taken together, the decrease in GSH, caused by NEFAs induced in earlier stages of oxidative stress, induced calcium release and further enhanced the sensitivity of calcium channels, Orai1. NF $\kappa$ B could be activated after Ca<sup>2+</sup> entry to enhance Orai1 expression and is thus part of a positive feedback further augmenting Ca<sup>2+</sup> influx (Eylenstein et al., 2012). Increased levels of mitochondrial Ca<sup>2+</sup> could increase ROS generation in mitochondria and further enhance ER stress.

## CONCLUSION

In conclusion, the present study is the first to clearly demonstrate the involvement of NEFA-sensitive NF $\kappa$ B–Orai1 signaling in the regulation of oxidative stress and ER stress in the pathological process of NAFLD; moreover, NF $\kappa$ B–Orai1 influences ROS generation and further enhances ER stress.

## DATA AVAILABILITY STATEMENT

All datasets generated for this study are included in the manuscript/**Supplementary Files**.

## ETHICS STATEMENT

The animal study was reviewed and approved by the animal experiments were conducted according to the Chinese law for the welfare of animal and were approved by Heilongjiang Bayi Agricultural University.

## AUTHOR CONTRIBUTIONS

BBZ, WY, and CXu designed the project. ML, YZ, HG, and BDZ performed the experiments and analyzed the results. CXi and HZ revised the manuscript. BBZ and ML drafted the manuscript. All authors revised the final version of the manuscript.

## REFERENCES

- Abdelmagid, S. A., Clarke, S. E., Nielsen, D. E., Badawi, A., El-Sohehy, A., Mutch, D. M., et al. (2015). Comprehensive profiling of plasma fatty acid concentrations in young healthy Canadian adults. *PLoS One* 10:e0116195. doi: 10.1371/journal.pone.0116195
- Cao, S. S., and Kaufman, R. J. (2014). Endoplasmic reticulum stress and oxidative stress in cell fate decision and human

## FUNDING

The work was supported by the National Natural Science Foundation of China (31702308 and 31672622), the National Program on Key Research Project of China (2016YFD0501206), the Youth Innovative Talent Program of Heilongjiang Bayi Agricultural University (CXRC2017015), and the Changjiang Scholars Program of the Chinese Ministry of Education (Q2017229).

## SUPPLEMENTARY MATERIAL

The Supplementary Material for this article can be found online at: <https://www.frontiersin.org/articles/10.3389/fcell.2019.00202/full#supplementary-material>

**FIGURE S1** | Phospho-p65 protein expressed in BRL-3A cells. **(A)** Original Western blots showing the protein expression of phospho-p65, NF $\kappa$ B p65, and  $\beta$ -actin in BRL-3A cells incubated without or with NEFA (1.2 mM, 12 h) in the absence or presence of Orai1 inhibitor BTP2; arithmetic means  $\pm$  SEM ( $n = 9$ ) of the phospho-p65/ $\beta$ -actin ratio in BRL-3A cells incubated without (white bar) or with (black bar) NEFA (1.2 mM, 12 h) in the absence (left bars) or presence (right bars) of Orai1 inhibitor BTP2; arithmetic means  $\pm$  SEM ( $n = 9$ ) of the NF $\kappa$ B p65/ $\beta$ -actin ratio in BRL-3A cells incubated without (white bar) or with (black bar) NEFA (1.2 mM, 12 h) in the absence (left bars) or presence (right bars) of Orai1 inhibitor BTP2. **(B)** Original Western blots showing the protein expression of phospho-p65, NF $\kappa$ B p65, and  $\beta$ -actin in BRL-3A cells incubated without or with NEFA (1.2 mM, 12 h) in the absence or presence of NF $\kappa$ B p65 inhibitor wogonin; arithmetic means  $\pm$  SEM ( $n = 9$ ) of the phospho-p65/ $\beta$ -actin ratio in BRL-3A cells incubated without (white bar) or with (black bar) NEFA (1.2 mM, 12 h) in the absence (left bars) or presence (right bars) of NF $\kappa$ B p65 inhibitor wogonin; arithmetic means  $\pm$  SEM ( $n = 9$ ) of the NF $\kappa$ B p65/ $\beta$ -actin ratio in BRL-3A cells incubated without (white bar) or with (black bar) NEFA (1.2 mM, 12 h) in the absence (left bars) or presence (right bars) of NF $\kappa$ B p65 inhibitor wogonin. **(C)** Original Western blots showing the protein expression of phospho-p65, NF $\kappa$ B p65, and  $\beta$ -actin in BRL-3A cells incubated without or with NEFA (1.2 mM, 12 h) in the absence or presence of siOrai1; arithmetic means  $\pm$  SEM ( $n = 9$ ) of the phospho-p65/ $\beta$ -actin ratio in BRL-3A cells incubated without (white bar) or with (black bar) NEFA (1.2 mM, 12 h) in the absence (left bars) or presence (right bars) of siOrai1; arithmetic means  $\pm$  SEM ( $n = 9$ ) of the NF $\kappa$ B p65/ $\beta$ -actin ratio in BRL-3A cells incubated without (white bar) or with (black bar) NEFA (1.2 mM, 12 h) in the absence (left bars) or presence (right bars) of siOrai1. \* $p < 0.05$ , \*\* $p < 0.01$  indicate significant difference from control; # $p < 0.05$ , ## $p < 0.01$ , ### $p < 0.001$  indicate significant difference from NEFAs alone (one-way ANOVA).

**FIGURE S2** | Effect of high-concentration NEFAs and siOrai1 on phospho-NF $\kappa$ B p65 localization in BRL-3A cells. Original immunofluorescence images demonstrating nuclear staining (blue; left images), phospho-NF $\kappa$ B p65 (red; middle images), and an overlaying of all nuclear staining and phospho-NF $\kappa$ B p65-specific antibody in BRL-3A cells incubated without (upper images) or with (second images) NEFAs (1.2 mM, 3 h), siOrai1 (third images), or siOrai1 + NEFAs (lower images). Scale bar: 25  $\mu$ m.

- disease. *Antioxid Redox Signal*. 21, 396–413. doi: 10.1089/ars.2014.5851
- Chan, C. M., Huang, D. Y., Huang, Y. P., Hsu, S. H., Kang, L. Y., Shen, C. M., et al. (2016). Methylglyoxal induces cell death through endoplasmic reticulum stress-associated ROS production and mitochondrial dysfunction. *J. Cell Mol. Med.* 20, 1749–1760. doi: 10.1111/jcmm.12893
- Czerwinska, J., Nowak, M., Wojtczak, P., Dziuban-Lech, D., Ciesla, J. M., Kolata, D., et al. (2018). ERCC1-deficient cells and mice are hypersensitive to lipid

- peroxidation. *Free Radic. Biol. Med.* 124, 79–96. doi: 10.1016/j.freeradbiomed.2018.05.088
- Del Rio, D., Stewart, A. J., and Pellegrini, N. (2005). A review of recent studies on malondialdehyde as toxic molecule and biological marker of oxidative stress. *Nutr. Metab. Cardiovasc. Dis.* 15, 316–328. doi: 10.1016/j.numecd.2005.05.003
- Diraison, F., Moulin, P., and Beylot, M. (2003). Contribution of hepatic de novo lipogenesis and reesterification of plasma non esterified fatty acids to plasma triglyceride synthesis during non-alcoholic fatty liver disease. *Diabetes Metab.* 29, 478–485. doi: 10.1016/s1262-3636(07)70061-7
- Donnelly, K. L., Smith, C. I., Schwarzenberg, S. J., Jessurun, J., Boldt, M. D., and Parks, E. J. (2005). Sources of fatty acids stored in liver and secreted via lipoproteins in patients with nonalcoholic fatty liver disease. *J. Clin. Invest.* 115, 1343–1351. doi: 10.1172/jci200523621
- Engin, A. (2017). Non-alcoholic fatty liver disease. *Adv. Exp. Med. Biol.* 960, 443–467. doi: 10.1007/978-3-319-48382-5\_19
- Eylenstein, A., Schmidt, S., Gu, S., Yang, W., Schmid, E., Schmidt, E. M., et al. (2012). Transcription factor NF-kappaB regulates expression of pore-forming Ca2+ channel unit. Orail, and its activator, STIM1, to control Ca2+ entry and affect cellular functions. *J. Biol. Chem.* 287, 2719–2730. doi: 10.1074/jbc.M111.275925
- Farmer, E. E., and Davoine, C. (2007). Reactive electrophile species. *Curr. Opin. Plant Biol.* 10, 380–386. doi: 10.1016/j.pbi.2007.04.019
- Giacomini, K. M., Swezey, S. E., Giacomini, J. C., and Blaschke, T. F. (1980). Administration of heparin causes in vitro release of non-esterified fatty acids in human plasma. *Life Sci.* 27, 771–780. doi: 10.1016/0024-3205(80)90331-8
- Gorlach, A., Klappa, P., and Kietzmann, T. (2006). The endoplasmic reticulum: folding, calcium homeostasis, signaling, and redox control. *Antioxid Redox Signal.* 8, 1391–1418. doi: 10.1089/ars.2006.8.1391
- Hasnain, S. Z., Prins, J. B., and McGuckin, M. A. (2016). Oxidative and endoplasmic reticulum stress in beta-cell dysfunction in diabetes. *J. Mol. Endocrinol.* 56, R33–R54. doi: 10.1530/JME-15-0232
- Hetherington, A. M., Sawyez, C. G., Zilberman, E., Stoianov, A. M., Robson, D. L., and Borradaile, N. M. (2016). Differential lipotoxic effects of palmitate and oleate in activated human hepatic stellate cells and epithelial hepatoma cells. *Cell. Physiol. Biochem.* 39, 1648–1662. doi: 10.1159/000447866
- Ivanova, H., Kerkhofs, M., La Rovere, R. M., and Bultynck, G. (2017). Endoplasmic reticulum–mitochondrial Ca(2+) fluxes underlying cancer cell survival. *Front. Oncol.* 7:70. doi: 10.3389/fonc.2017.00070
- Joy, S., Alikunju, A. P., Jose, J., Sudha, H. S. H., Parambath, P. M., Puthiyedathu, S. T., et al. (2017). Oxidative stress and antioxidant defense responses of *Etropilus suratensis* to acute temperature fluctuations. *J. Therm. Biol.* 70, 20–26. doi: 10.1016/j.jtherbio.2017.10.010
- Lang, F., Eylenstein, A., and Shumilina, E. (2012). Regulation of Orail/STIM1 by the kinases SGK1 and AMPK. *Cell Calcium.* 52, 347–354. doi: 10.1016/j.ceca.2012.05.005
- Lang, F., and Shumilina, E. (2013). Regulation of ion channels by the serum- and glucocorticoid-inducible kinase SGK1. *FASEB J.* 27, 3–12. doi: 10.1096/fj.12-218230
- Li, P., Liu, Y., Zhang, Y., Long, M., Guo, Y., Wang, Z., et al. (2013). Effect of non-esterified fatty acids on fatty acid metabolism-related genes in calf hepatocytes cultured in vitro. *Cell. Physiol. Biochem.* 32, 1509–1516. doi: 10.1159/000356588
- Moore, K., and Roberts, L. J. II (1998). Measurement of lipid peroxidation. *Free Radic. Res.* 28, 659–671.
- Ortiz de Orue Lucana, D., Wedderhoff, I., and Groves, M. R. (2012). ROS-mediated signalling in bacteria: zinc-containing Cys-X-X-Cys redox centres and iron-based oxidative stress. *J. Signal. Transduct.* 2012, 605905. doi: 10.1155/2012/605905
- Owen, J. B., and Butterfield, D. A. (2010). Measurement of oxidized/reduced glutathione ratio. *Methods Mol. Biol.* 648, 269–277. doi: 10.1007/978-1-60761-756-3\_18
- Plos One Staff. (2015). Correction: comprehensive profiling of plasma fatty acid concentrations in young healthy Canadian adults. *PLoS One* 10:e0128167. doi: 10.1371/journal.pone.0128167
- Prakriya, M., Feske, S., Gwack, Y., Srikanth, S., Rao, A., and Hogan, P. G. (2006). Orail is an essential pore subunit of the CRAC channel. *Nature* 443, 230–233. doi: 10.1038/nature05122
- Su, S., Wu, G., Cheng, X., Fan, J., Peng, J., Su, H., et al. (2018). Oleonic acid attenuates PCBs-induced adiposity and insulin resistance via HNF1b-mediated regulation of redox and PPARgamma signaling. *Free Radic. Biol. Med.* 124, 122–134. doi: 10.1016/j.freeradbiomed.2018.06.003
- Zeeshan, H. M., Lee, G. H., Kim, H. R., and Chae, H. J. (2016). Endoplasmic reticulum stress and associated ROS. *Int. J. Mol. Sci.* 17:327. doi: 10.3390/ijms17030327
- Zeng, L., Tang, W. J., Yin, J. J., and Zhou, B. J. (2014). Signal transductions and nonalcoholic fatty liver: a mini-review. *Int. J. Clin. Exp. Med.* 7, 1624–1631.
- Zhang, B., Yang, W., Zou, Y., Li, M., Guo, H., Zhang, H., et al. (2018). NEFA-sensitive orail expression in regulation of de novo lipogenesis. *Cell. Physiol. Biochem.* 47, 1310–1317. doi: 10.1159/000490226
- Zitka, O., Skalickova, S., Gumulec, J., Masarik, M., Adam, V., Hubalek, J., et al. (2012). Redox status expressed as GSH:GSSG ratio as a marker for oxidative stress in paediatric tumour patients. *Oncol. Lett.* 4, 1247–1253. doi: 10.3892/ol.2012.931

**Conflict of Interest:** The authors declare that the research was conducted in the absence of any commercial or financial relationships that could be construed as a potential conflict of interest.

Copyright © 2019 Zhang, Li, Zou, Guo, Zhang, Xia, Zhang, Yang and Xu. This is an open-access article distributed under the terms of the Creative Commons Attribution License (CC BY). The use, distribution or reproduction in other forums is permitted, provided the original author(s) and the copyright owner(s) are credited and that the original publication in this journal is cited, in accordance with accepted academic practice. No use, distribution or reproduction is permitted which does not comply with these terms.